applied sciences

MDPI

Article

Sustainable Photocatalytic Reduction of Maleic Acid: Enhancing Cu_xO/ZnO Stability with Polydopamine

Francesca Coccia [1,*], Andrea Mascitti [2], Giorgia Rastelli [3], Nicola d'Alessandro [4,5,6] and Lucia Tonucci [1]

[1] Department of Socio-Economic, Managerial and Statistical Studies, "G. d'Annunzio" University of Chieti-Pescara, Viale Pindaro 42, 65127 Pescara, Italy; lucia.tonucci@unich.it
[2] Department of Engineering and Geology, "G. d'Annunzio" University of Chieti-Pescara, Viale Pindaro 42, 65127 Pescara, Italy; andrea.mascitti@alumni.unich.it
[3] Department of Neuroscience, Imaging and Clinical Science, "G. d'Annunzio" University of Chieti-Pescara, Via dei Vestini, 31, 66100 Chieti, Italy; giorgia.rastelli@unich.it
[4] Department of Science, "G. d'Annunzio" University of Chieti-Pescara, Via dei Vestini, 31, 66100 Chieti, Italy; nicola.dalessandro@unich.it
[5] TEMA Research Center, "G. d'Annunzio" University of Chieti-Pescara, 66100 Chieti, Italy
[6] UdA-TechLab Research Center, "G. d'Annunzio" University of Chieti-Pescara, 66100 Chieti, Italy
* Correspondence: francesca.coccia@unich.it

Abstract: The development of effective photocatalysts for environmental applications is still a critical aspect of green chemistry. This study explores copper oxide (Cu_xO) catalysts supported on titanium dioxide (TiO_2) and zinc oxide (ZnO) for the photocatalytic reduction of maleic acid to succinic acid under ultraviolet (UV) light in water. The main goal was to evaluate the performance of CuO/ZnO compared to CuO/TiO_2 in photoreduction. In order to improve the efficiency of the first catalyst, an environmentally friendly synthesis, assisted by polydopamine (PDA), was tested, obtaining the Cu_2O/ZnO-PDA catalyst. The results showed that CuO/TiO_2 exhibited the highest activity for maleic acid reduction, obtaining a succinic acid yield and a selectivity of 32% after 24 h of reaction time, but comparable results could be reached even with Cu_2O/ZnO-PDA increasing the reaction time. Furthermore, the addition of sodium ascorbate as a co-catalyst in the reaction mixture allowed us to overtake the previous results, leading to a succinic acid yield of 61% and a selectivity of 67%. These findings suggest that the PDA shell can be a solution for Cu_xO photodegradation, making Cu_2O/ZnO-PDA an alternative to the toxic CuO/TiO_2.

Keywords: succinic acid; copper oxides; polydopamine

Academic Editor: Fabrizio Medici

Received: 7 January 2025
Revised: 28 January 2025
Accepted: 4 February 2025
Published: 6 February 2025

Citation: Coccia, F.; Mascitti, A.; Rastelli, G.; d'Alessandro, N.; Tonucci, L. Sustainable Photocatalytic Reduction of Maleic Acid: Enhancing Cu_xO/ZnO Stability with Polydopamine. *Appl. Sci.* **2025**, *15*, 1631. https://doi.org/10.3390/app15031631

1. Introduction

Maleic acid (MA) is a dicarboxylic acid with a conjugated double bond that can undergo several transformations in a reducing environment; it can isomerize to fumaric acid (FA) under certain conditions (thermal, catalytic, or photo-induced); this geometric isomerization occurs because FA is thermodynamically more stable [1]. The partial reduction of MA can produce intermediates such as maleic anhydride [2], depending on the reducing system used; moreover, the double bond of MA can be cleaved by radical species or further functionalized, leading to, for example, malic acid [3]. Another reductive transformation is the hydrogenation of the C-C double bond, producing succinic acid (SA) [4]. The reduction of MA to SA has garnered significant attention due to the potential of SA as a valuable building block for a wide range of industrial applications [5], including the synthesis of biodegradable polymers, solvents, and other fine chemicals [6]. The growing demand for

sustainable processes in chemical synthesis has driven considerable interest in the development of green catalytic systems to produce key platform chemicals. The production of SA is typically achieved through petrochemical routes [7] or the use of stoichiometric reducing agents, raising concerns about environmental sustainability; additionally, it often requires high-pressure conditions or catalysts, such as Pd and Pt, with stoichiometric formic acid as a reducing agent [4].

Photocatalysis offers a sustainable alternative for reducing MA to SA using solar or UV light under mild conditions [8]. Catalysts, like TiO_2 [8] and graphitic carbon nitride (g-C_3N_4) [9], have been effective in aqueous phase reactions. TiO_2 has demonstrated its higher stability, efficient charge separation, and strong oxidative potential; however, its classification as a potential carcinogen [10] has shifted interest toward safer alternatives like ZnO [11]. ZnO and TiO_2 have some similarities, such as a wide bandgap and strong UV light absorption. However, ZnO has limitations related to faster electron–hole recombination [12], but doping it with metal or non-metal species [13] can achieve performance comparable to TiO_2 [11].

This study focuses on Cu_xO-based photocatalysts supported on TiO_2 and ZnO. CuO is a promising material [14] due to its narrow bandgap (1.2–1.7 eV) [15], visible light absorption [16], and cost-effectiveness. The application is limited, for example, by photodegradation since it represents a significant drawback for CuO and Cu_2O-based photocatalysts; photoinduced charge carriers oxidize the material into less active species, leading to reduce efficiency and durability [17,18]. Protective strategies, such as heterostructures like CuO/TiO_2, employ a Z-scheme charge transfer mechanism [19]; this structure enhances charge separation by efficiently directing photogenerated electrons and holes to different composite regions, reducing oxidative stress on Cu_2O. This mechanism also prevents the accumulation of holes on the Cu_2O surface, which is a key factor in driving photodegradation. Even an appropriate surface modification [20] can help overcome the photodegradation problem. A protective surface coating with, for example, polydopamine (PDA) can offer a dual benefit [21]: this kind of robust coating on the catalyst surface provides physical protection against oxidative species; additionally, PDA's redox-active functional groups (e.g., catechol and amine groups) scavenge reactive oxygen species generated during the reaction, further mitigating photodegradation. Finally, the PDA shell improves the charge separation at the CuO/ZnO interface, facilitating electron transfer and reducing recombination rates of photogenerated carriers [22]. While not inherently photoactive, PDA can enhance photocatalytic performance when combined with semiconductors. This facilitates better charge separation and reduces electron–hole recombination by modifying the catalyst surface, enhancing its optical and electronic properties [23–25]. This phenomena lead to greater photocatalytic efficiency while simultaneously addressing stability concerns [26].

Here, Cu_2O/ZnO-PDA and CuO/ZnO, recently synthesized in our research group to make antibacterial materials [27], work as photocatalysts under UV light (λ = 254 nm) in the reduction of MA to SA, leveraging water as both the solvent and reducing agent, making the process more sustainable. The use of the catalytic amount of sodium ascorbate in the reaction mixture increased both the yield and the selectivity. Ascorbate is a well-known electron donor [28], frequently employed in photoinduced electron transfer experiments conducted in aqueous environments [29]; often utilized as a sacrificial electron donor, ascorbate generates a radical species with a relatively long lifetime, which can efficiently participate in electron transfer processes [30].

The study highlights the potential of ZnO as a safer support, emphasizing the need for strategies to overcome its lower stability and faster recombination rates compared to TiO_2.

2. Materials and Methods

Sodium lignosulphonate was a gift from Burgo Group S.p.A., Tolmezzo (UD, Italy); ethyl alcohol and acetonitrile were purchased from Carlo Erba Reagents, Cornaredo (MI, Italy). $Cu_2O \geq 97\%$ was bought from VWR, Milan (Italy). All the other chemicals were purchased from Merck and used without any purification.

2.1. Instruments

The sonicator equipped with the probe was a Ultrasonic Processor GEX 400, Cole Parmer, Vernon Hills (IL, USA), set at an 80% amplitude.

XRD analysis was performed on a Miniflex II Rigaku automated power XRD system (Cu Kα radiation, 45 kV, 100 mA), Rigaku Corporation, Osaka, Japan. Diffraction data were recorded using continuous scanning at 3° min^{-1}, with 0.010° steps. The identification of component samples was performed using Match! Software version 3.15 and the Crystallography open database (COD 2023). The samples were dried and ground in a mortar to obtain a powder; only Cu_2O/ZnO-PDA was previously washed with water since the presence of salts deriving from synthesis hid the XRD profile of the sample.

TEM analyses were performed with a 120 kV JEM-1400 Flash Transmission Electron Microscope (Jeol Ltd., Tokyo, Japan) equipped with a CMOS camera Matataki and TEM Center software (Jeol Ltd., Tokyo, Japan). The samples were prepared using 5 mL of a 10 mg catalyst solution in 30 mL ultrapure water. The solution was sonicated in an ultrasonic bath for 3 min; then, it was deposited onto 3 mm carbon films on 300 mesh grids made of copper (Agar Scientific Ltd., Rotherham, UK), and the solvent was left to evaporate for a few hours at room temperature. The size and shape were determined from electron micrographs of non-overlapping regions randomly collected using the TEM Center Software (SightX Viewer Ver.2.1.23.1656); the diameter of the nanoparticles (NPs) was determined as an average from 50 individual NPs.

NMR spectra were obtained using a 300 spectrometer (7.05 Tesla), Bruker Avance Billerica, (MA, USA), equipped with a high-resolution multinuclear probe operating in the range of 30 MHz to 300 MHz. To eliminate the dominant water signal in the ^1H NMR spectra, water suppression was carried out using a presaturation sequence of a composite pulse (zgcppr Bruker sequence). A co-axial capillary tube that contained a 30 mM D_2O solution of 3-(trimethylsilyl)propionic-2,2,3,3-d_4 acid, sodium salt, was used as the reference.

The gas chromatography–mass spectroscopy (GC-MS) apparatus comprised a Thermo Scientific, Waltham (MA, USA) Focus series gas chromatograph coupled to an ISQ mass-selective detector equipped with a split–splitless injection system (injections made in splitless mode) and an HP5 MS (cross-linked 5% phenyl methyl siloxane) capillary column (15 m length, 0.25 mm diameter, 0.1 μm film thickness) using helium as carrier gas at constant pressure of 50 kPa. The photochemical multiray apparatus assembled by Helios Italquartz Srl, Cambiago (MI, Italy) was used for photochemical reactions, which contained ten UV lamps of 15 W power each that emit light centered at 254 nm.

2.2. Catalysts Preparation

CuO/TiO_2 (1% Cu wt%) was synthesized by impregnating TiO_2 (P25) with $Cu(NO_3)_2$ in water, followed by ultrasonication for 1 h and stirring at 95 °C for 4 h; then, the mixture was filtrated and calcinated at 150 °C for 2 h and finally at 500 °C for 30 min [31].

CuO/ZnO (3% Cu wt%). ZnO NPs were prepared by a modified protocol using sodium lignosulphonate as described in the previous articles [27,32,33]: 1 g of $Zn(CH_3COO)_2 \cdot 2H_2O$, 0.8 g of sodium lignosulphonate, and 0.36 g of NaOH were dissolved in 50 mL of ethyl alcohol; the solution was left at 80 °C for 12 h; the obtained precipitate was filtered, washed

with water and ethyl alcohol, and finally calcined at 700 °C for 4 h in air. A portion of synthesized ZnO NPs (0.1 g) was dispersed in 20 mL of water, and 0.012 g of $CuSO_4 \cdot 5H_2O$ was added; the solution was kept at 100 °C for 12 h, and finally, the precipitate was filtered and washed with water and ethyl alcohol and then calcined at 400 °C for 4 h in air [34].

Cu_2O/ZnO-PDA (71 mg/L of Cu) was synthesized similarly as reported in the previous article [27], and 0.32 g of dopamine hydrochloride was dissolved in 20 mL of water and sonicated with the probe sonicator for 5 min. Then, 0.4 g of $Zn(CH_3COO)_2 \cdot 2H_2O$ and 0.012 g of $CuSO_4 \cdot 5H_2O$, dissolved in 20 mL of water, were added to the dopamine solution; the mixture was sonicated for 5 min; finally, its pH was adjusted at 8 with a NaOH solution (final solution volume of 43 mL) then sonicated for a further 5 min while cooling the container with ice [35].

2.3. Reduction Procedure

An amount of 13 mg of CuO/ZnO was added to 120 mL of MA aqueous solution 70 mM (0.07% molar ratio Cu/MA). An amount of 13 mg of CuO/TiO_2 was added to 40 mL of MA aqueous solution 70 mM (0.07% molar ratio Cu/MA). The reaction was tested even modifying the pH of the reaction mixture to 8 with NaOH solution. An amount of 880 µL of Cu_2O/ZnO-PDA solution was added to 20 mL of MA aqueous solution 70 mM (0.07% molar ratio Cu/MA). An amount of 49 mg of MA was added to 15 mL of $CuSO_4$ aqueous solution 0.02 mM (0.07% molar ratio Cu/MA). An amount of 5 mg of Cu_2O was added to 10 mL of MA aqueous solution 100 mM (0.7% molar ratio Cu/MA). And an amount of 12 mg of ZnO was added to 120 mL of MA aqueous solution 70 mM.

The photocatalytic reduction of MA was carried out in quartz test tubes sealed with rubber stoppers and flushed for 15 min with N_2 to eliminate air. The reaction mixture, containing the catalyst and the substrate in an aqueous solution, was irradiated under UV light (λ = 254 nm). The reactions were conducted at room temperature (30 °C) for 24–120 h. At the end of the reaction, the reaction mixture was centrifuged at 3000 rpm for 3 min. The supernatant solution was collected and subjected to NMR analysis to identify the products (Figures S2–S11).

3. Results and Discussion

Two copper oxide-based catalysts supported on ZnO were prepared and compared to CuO/TiO_2, a photocatalyst widely recognized for its superior photocatalytic efficiency [36]. However, concerns over the potential health risks related to TiO_2 [10] have driven the exploration of alternative materials [37], arousing interest in developing less hazardous photocatalyst supports, such as ZnO.

CuO/TiO_2 was synthesized by the impregnation method, as reported in the literature [31], yielding the copper-doped titania catalyst. The CuO/ZnO catalyst, instead, was synthesized in two steps; first, ZnO NPs were prepared using sodium lignosulfonate, a by-product of the paper industry, as a template for NPs; then, these NPs were doped with copper (II) salt and calcined. The resulting catalyst was characterized using XRD and TEM. XRD revealed a pattern with characteristic signals attributable to the hexagonal wurtzite structure of ZnO, which were not influenced by the small amount of copper oxide present, likely undetectable due to the sensitivity limits of the technique (Figure S1A) [27]. TEM images showed the approximately spherical shape of the CuO/ZnO NPs with dimensions of 25 ± 11 nm (Figure 1A).

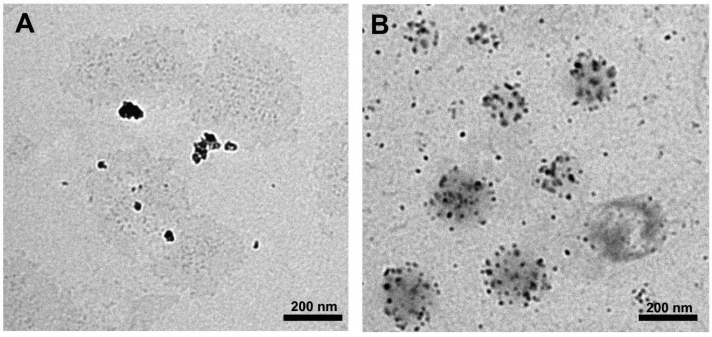

Figure 1. TEM images of (**A**) CuO/ZnO NPs and (**B**) Cu_2O/ZnO-PDA NPs embedded in PDA shell. Scale bar: 200 nm.

Another catalyst, composed of Cu_2O and ZnO, was prepared using a natural shell of PDA synthesized from dopamine hydrochloride in a basic solution (Cu_2O/ZnO-PDA). The synthesis of Cu_2O-doped ZnO NPs embedded in a PDA shell was easily carried out in 15 min in a water solution using a probe sonicator. This solution containing the photocatalyst was characterized by XRD and TEM [27]; the diffractogram showed broad peaks attributable to ZnO; the signals of copper oxide were not visible due to the low Cu_2O amount (Figure S1B). To investigate the oxidation state of copper oxide, the same synthesis was performed without the addition of Zn (using dopamine hydrochloride and $CuSO_4 \cdot 5H_2O$ as starting materials) [27] since the reduction of $CuSO_4$ is not influenced by the presence of Zn [38], as it is driven by the reducing properties of PDA [39]. The XRD analysis revealed the characteristic signals of Cu_2O (broad peaks at 2θ values of 37°, 42°, and 61°) [40] (Figure S1C). TEM images showed Cu_2O/ZnO-PDA NPs as a uniform distribution of spherical particles with an average diameter of 14 ± 2 nm, mostly encapsulated within PDA shells measuring 230 nm in size (Figure 1B).

Initial tests were conducted by irradiating aqueous solutions of MA with 254 nm light in the presence of the photocatalysts.

The best results were observed with CuO/TiO_2 at 0.5% molar ratio Cu/reagent, achieving a 32% yield of SA after 24 h of reaction time with 32% selectivity at full reagent conversion; it is assumed that other products, undetectable by NMR, have been formed. The results were not improved by longer reaction times as the catalyst loses its activity over extended periods, as observed in MA reduction reactions carried out over 24 h under the same conditions reported above; further pH modifications of the reaction mixture were tested, but they did not influence the results of the reaction. Instead, the presence of air in the reactor inhibited the reaction, leading to only FA as the product (32% yield); so, it is crucial to conduct the process under an inert N_2 atmosphere.

The CuO/ZnO catalyst was active in the reduction of MA to SA, producing 10% of yield after 24 h (47% yield of FA with 57% of MA conversion), thus exhibiting a lower catalytic efficiency compared to CuO/TiO_2, which led to 32% of SA yield with a total MA conversion (FA was not observed). CuO/TiO_2 was superior in selectivity, reaching 32%, while CuO/ZnO only achieved 17%.

To enhance the catalytic performance of CuO/ZnO, the reaction time should be extended. However, our experimental data have shown that the catalytic activity of CuO/ZnO is limited to short reaction times, as CuO is susceptible to photodegradation. So, synthesizing a strong CuO-based catalyst that can endure prolonged UV irradiation is crucial for its successful application in photochemical processes. Maintaining its structural integrity and active sites while achieving high conversion and selectivity is crucial for a durable catalyst.

To deal with this, a protective PDA shell was applied to the CuO/ZnO catalyst. PDA, derived from the natural oxidation of dopamine, was selected because of its many advantages: it is eco-friendly, exhibits strong adhesion to various substrates, is easy to synthesize under mild conditions, and provides chemical stability [41,42]. The synthesis of the Cu_2O/ZnO-PDA catalyst was sustainably performed in water using an ultrasonic processor with an immersion probe, taking only 15 min. The presence of PDA with its catecholamine moiety [43], during synthesis, led to the reduction of copper (II) to copper (I) (obtaining Cu_2O), as demonstrated in the previous article [27].

Even Cu_2O/ZnO-PDA was used in the photoreduction of MA to SA, yielding 9% of SA with a selectivity of 15% after 24 h of reaction time (the secondary product was FA with a yield of 24% and a selectivity of 40%), 17% of SA with a selectivity of 24% after 48 h (FA 19% with a selectivity of 27%), and 25% of SA with a selectivity of 27% after 72 h (FA 7% with a selectivity of 8%). These results were comparable to those obtained in the presence of CuO/TiO_2 (32% of SA yield with 32% of SA selectivity after 24 h) (Table 1 and Figure 2).

Table 1. Conversion of MA and yield in SA during the time (24, 48, and 72 h) of aqueous MA photoreduction reaction, employing Cu_2O/ZnO-PDA as photocatalyst under 254 nm.

Reaction Time (h)	% SA Yield (mol/mol)	% FA Yield (mol/mol)	% MA Conversion (mol/mol)
24	9	24	60
48	17	19	70
72	25	7	92

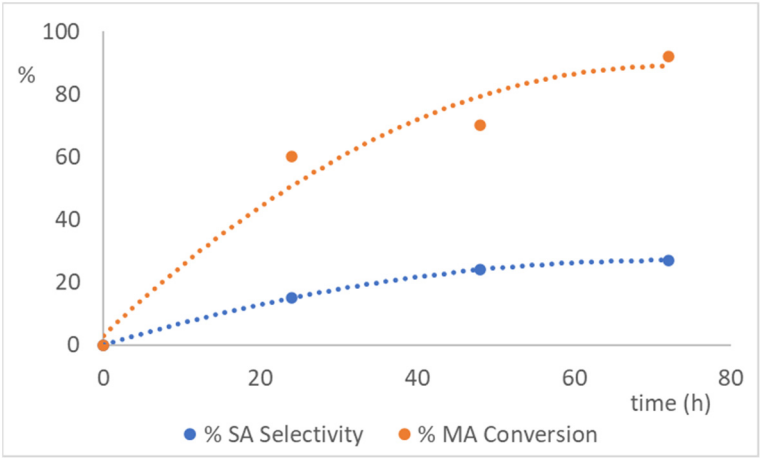

Figure 2. Conversion of MA and selectivity to SA during the time (24, 48, and 72 h) of aqueous MA photoreduction reaction, employing Cu_2O/ZnO-PDA as photocatalyst under 254 nm.

Despite light exposure, the PDA-coated catalyst remained efficient over 72 h, consistently yielding 25% SA.

Sodium ascorbate, a sustainable and biocompatible reducing agent [44], was added to the reaction system to further enhance reaction outcomes. Sodium ascorbate offers several advantages: it is non-toxic, water-soluble, and compatible with green chemistry principles. When added in equimolar amount relative to the substrate, significant improvements were observed; after 72 h, the reaction achieved 78% yield of SA with excellent selectivity of 78%.

A test was conducted in deuterated water to determine whether the ascorbate was the direct hydrogen donor for the substrate or if the hydrogen came from the water, as initially intended. In the D_2O experiment, the conversion of MA (20%) was observed by the ^1H NMR spectrum, but the signal corresponding to SA was found with an integration value equal to half of that observed when the experiment was carried out in water (Figure S11);

this suggested the formation of the deuterated SA (yield 18%), confirmed by GC-MS analysis, which identified a molecular mass signal corresponding to that of SA + 2. These results imply that sodium ascorbate is not the direct hydrogen donor but acts as a radical initiator, promoting electron transfer in the reaction; in fact, the photolysis of ascorbic acid in an inert atmosphere and water can result in the formation of radicals, like ascorbate radicals and superoxide radicals [45,46]. More research is needed to define the actual mechanism of the reaction.

To assess the ascorbate efficiency as a co-catalyst, its amount was reduced, employing a substrate-to-ascorbate ratio of 1:5.5. This adjustment yielded comparable results to those obtained with equimolar ascorbate relative to the substrate. The reaction achieved a 26% SA yield with a selectivity of 57% after 24 h of reaction time, a 45% SA yield with the same selectivity after 48 h, and a 61% SA yield with 67% selectivity after 72 h (Figure 3).

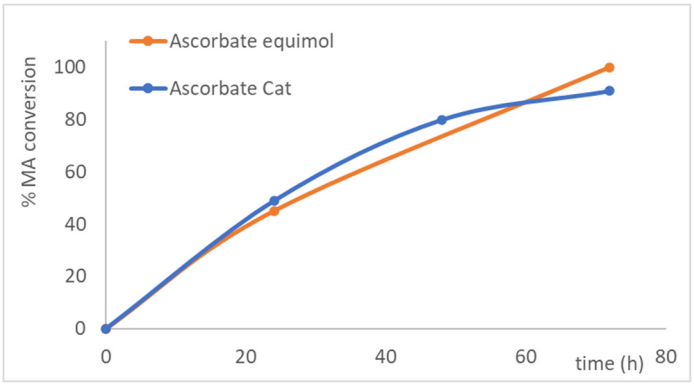

(**a**)

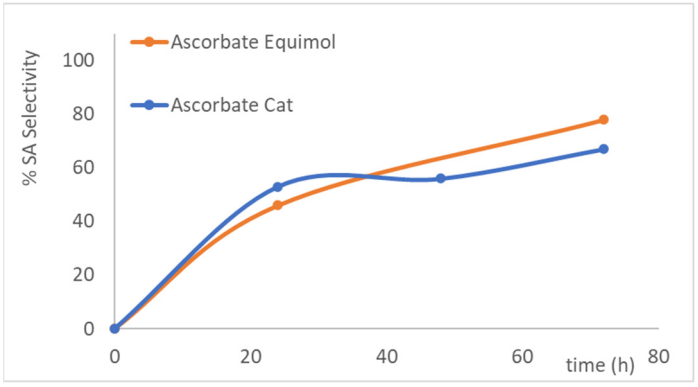

(**b**)

Figure 3. (**a**) Conversion of MA during the time in photoreduction reaction catalyzed by Cu_2O/ZnO-PDA in the presence of sodium ascorbate as co-catalyst or added in equimolar ratio to MA. (**b**) Selectivity to SA during the time in MA photoreduction reaction catalyzed by Cu_2O/ZnO-PDA in the presence of sodium ascorbate as co-catalyst or added in equimolar ratio to MA.

These results demonstrated that Cu_2O/ZnO-PDA, when combined with optimized ascorbate amount, achieves catalytic performance better than the benchmark CuO/TiO_2 along 72 h of reaction time. Analyzing the data reported in Figure 4, an initial production of FA from MA was observed, accompanied by a simultaneous reduction to SA, while the selectivity for the desired product remains comparable throughout the reaction time, suggesting that the initial reaction step involves the isomerization of MA to FA (step not catalyzed), followed by subsequent catalyzed reduction to SA [47] (Figure 5).

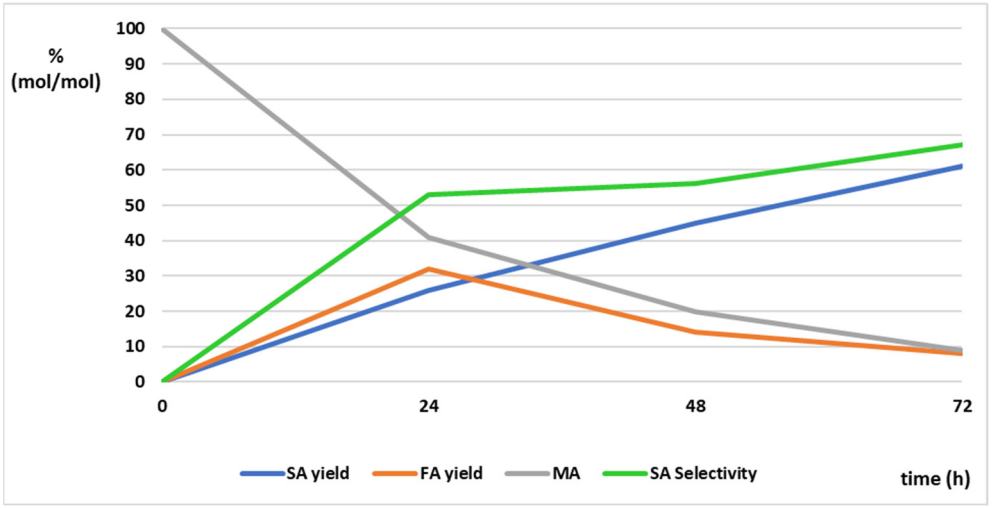

Figure 4. Conversion and yields during aqueous MA photoreduction to SA employing Cu_2O/ZnO-PDA as photocatalyst and sodium ascorbate as co-catalyst under 254 nm.

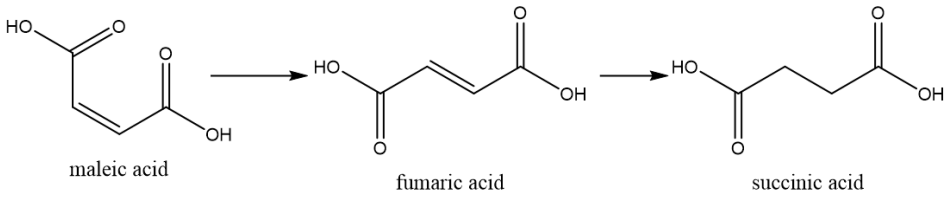

Figure 5. Reaction scheme of MA conversion to FA and SA.

The effectiveness of the newly prepared catalyst was supported by conducting control reactions using its individual components (ZnO, Cu_2O, or $CuSO_4$) as photocatalysts under identical reaction conditions. These tests yielded no SA and only resulted in a conversion to FA (32% after 12 h).

The tuned system was able to overcome the copper oxide photodegradation problem thanks to the presence of a PDA shell around the photocatalyst, and it can boast high selectivity in the reduction reaction of MA to SA thanks to the presence of ascorbate in the co-catalytic amount. Extending the lifespan of the catalyst exposed to UV light, and thereby the reaction times, can result in higher yields while aligning with the principles of green chemistry.

4. Conclusions

ZnO was chosen as an alternative semiconductor to TiO_2 and doped with copper oxides to improve catalytic efficiency. However, the proposed catalysts, which were less efficient than CuO/TiO_2, required longer reaction times, which were hindered by the photodegradation of Cu_xO. As a result, it was not possible to achieve outcomes comparable to those obtained with CuO/TiO_2. To address this, the catalyst was protected with a PDA shell to extend its lifespan, thus maintaining activity beyond 72 h of reaction. This allowed the catalyst to produce results comparable to the reference material. Furthermore, adding a co-catalytic amount of sodium ascorbate increased the reaction selectivity, achieving significantly higher yields and selectivities for SA compared to the TiO_2-based reference system. Incorporating PDA as a protective shell represents a promising strategy to address the photodegradation of copper oxide-based catalysts. By leveraging sustainable materials and improving catalyst durability, this work contributes to the development of more environmentally friendly photocatalytic systems, able to produce SA from MA in water with catalytic sodium ascorbate amount under UV light. In this way, it was possible to

obtain a SA yield of 61% with a selectivity of 67%. Studies on the reaction mechanism to have experimental evidence on the role of ascorbate will need to be conducted.

Supplementary Materials: The following supporting information can be downloaded at https://www.mdpi.com/article/10.3390/app15031631/s1, Figure S1: XRD pattern of CuO/ZnO (A) and Cu_2O/ZnO-PDA (B); Figure S2: ^{1}HNMR photoreduction of MA carried out in H_2O without any catalyst at 0 h reaction time; Figure S3: ^{1}HNMR photoreduction of MA carried out in H_2O without any catalyst at 12 h reaction time; Figure S4: ^{1}HNMR photoreduction of MA carried out in H_2O employing the catalyst Cu_2O/ZnO-PDA with equimolare sodium ascorbate at 0 h reaction time; Figure S5: ^{1}HNMR photoreduction of MA carried out in H_2O employing the catalyst Cu_2O/ZnO-PDA with equimolare sodium ascorbate at 24 h reaction time; Figure S6: ^{1}HNMR photoreduction of MA carried out in H_2O employing the catalyst Cu_2O/ZnO-PDA with equimolare sodium ascorbate at 72 h reaction time; Figure S7: ^{1}HNMR photoreduction of MA carried out in H_2O employing the catalyst Cu_2O/ZnO-PDA with sodium ascorbate in co-catalytic amount at 0 h reaction time; Figure S8: ^{1}HNMR photoreduction of MA carried out in H_2O employing the catalyst Cu_2O/ZnO-PDA with sodium ascorbate in co-catalytic amount at 24 h reaction time; Figure S9: ^{1}HNMR photoreduction of MA carried out in H_2O employing the catalyst Cu_2O/ZnO-PDA with sodium ascorbate in co-catalytic amount at 48 h reaction time; Figure S10: ^{1}HNMR photoreduction of MA carried out in H_2O employing the catalyst Cu_2O/ZnO-PDA with sodium ascorbate in co-catalytic amount at 72 h reaction time; Figure S11: ^{1}HNMR photoreduction of MA carried out in D_2O employing the catalyst Cu_2O/ZnO-PDA with sodium ascorbate in co-catalytic amount at 24 h reaction time.

Author Contributions: Conceptualization, F.C. and L.T.; methodology, F.C.; investigation, F.C., A.M. and G.R.; data curation, F.C.; writing—original draft preparation, F.C. and A.M.; writing—review and editing, N.d. and L.T.; supervision, N.d. and L.T.; project administration, L.T.; funding acquisition, L.T. All authors have read and agreed to the published version of the manuscript.

Funding: The research project was partially supported by the FSE-REACT-EU, PON Ricerca e innovazione 2014-2020 DM 1062/202, Cod: MUR 53-G-14753.

Institutional Review Board Statement: Not applicable.

Informed Consent Statement: Not applicable.

Data Availability Statement: The data are available upon request due to restrictions. The data presented in this study are available upon request from the corresponding author.

Acknowledgments: The authors acknowledge the CAST—Center for Advanced Studies and Technology of Chieti for supplying the cryogenic gases.

Conflicts of Interest: The authors declare no conflicts of interest.

References

1. Gao, Z.; Chen, W.; Chen, X.; Wang, D.; Yi, S. Study on the Isomerization of Maleic Acid to Fumaric Acid without Catalyst. *Bull. Korean Chem. Soc.* **2018**, *39*, 920–924. [CrossRef]
2. Calkin, H.L. United States Patent Office. *Palimpsest* **1969**, *50*, 369–373. [CrossRef]
3. Kövilein, A.; Kubisch, C.; Cai, L.; Ochsenreither, K. Malic Acid Production from Renewables: A Review. *J. Chem. Technol. Biotechnol.* **2020**, *95*, 513–526. [CrossRef]
4. López Granados, M.; Moreno, J.; Alba-Rubio, A.C.; Iglesias, J.; Martín Alonso, D.; Mariscal, R. Catalytic Transfer Hydrogenation of Maleic Acid with Stoichiometric Amounts of Formic Acid in Aqueous Phase: Paving the Way for More Sustainable Succinic Acid Production. *Green Chem.* **2020**, *22*, 1859–1872. [CrossRef]
5. Muzumdar, A.V.; Sawant, S.B.; Pangarkar, V.G. Reduction of Maleic Acid to Succinic Acid on Titanium Cathode. *Org. Process Res. Dev.* **2004**, *8*, 685–688. [CrossRef]
6. Delhomme, C.; Weuster-Botz, D.; Kühn, F.E. Succinic Acid from Renewable Resources as a C4 Building-Block Chemical—A Review of the Catalytic Possibilities in Aqueous Media. *Green Chem.* **2009**, *11*, 13–26. [CrossRef]

7. Mitrea, L.; Teleky, B.E.; Nemes, S.A.; Plamada, D.; Varvara, R.A.; Pascuta, M.S.; Ciont, C.; Cocean, A.M.; Medeleanu, M.; Nistor, A.; et al. Succinic Acid—A Run-through of the Latest Perspectives of Production from Renewable Biomass. *Heliyon* **2024**, *10*, e25551. [CrossRef] [PubMed]
8. Bellardita, M.; Virtù, D.; Di Franco, F.; Loddo, V.; Palmisano, L.; Santamaria, M. Heterogeneous Photocatalytic Aqueous Succinic Acid Formation from Maleic Acid Reduction. *Chem. Eng. J.* **2022**, *431*, 134131. [CrossRef]
9. Bashiri, M.; Hosseini-Sarvari, M. Synergic Effect of FeIII/g-C3N4 as Photocatalyst for Switchable Alteration of Furfural to Succinic Acid as Well as Maleic Acid: A Promising Approach for Sustainable Chemical Conversion and Advanced Environmental Remediation. *Biomass Bioenergy* **2024**, *191*, 107456. [CrossRef]
10. IARC. IARC Monographs on the Evaluation of Carcinogenic Risks to Humans. *IARC Monogr. Eval. Carcinog. Risks Hum.* **2010**, *93*, 9–38. [CrossRef]
11. Türkyılmaz, Ş.Ş.; Güy, N.; Özacar, M. Photocatalytic Efficiencies of Ni, Mn, Fe and Ag Doped ZnO Nanostructures Synthesized by Hydrothermal Method: The Synergistic/Antagonistic Effect between ZnO and Metals. *J. Photochem. Photobiol. A Chem.* **2017**, *341*, 39–50. [CrossRef]
12. Sanusi, I.; Almquist, C.B. ZnO/TiO_2 Composite Thin-Film Photocatalysts for Gas-Phase Oxidation of Ethanol. *Catalysts* **2023**, *13*, 1203. [CrossRef]
13. Soussi, A.; Haounati, R.; Ait hssi, A.; Taoufiq, M.; Asbayou, A.; Elfanaoui, A.; Markazi, R.; Bouabid, K.; Ihlal, A. First Principle Study of Structural, Electronic, Optical Properties of Co-Doped ZnO. *J. Compos. Sci.* **2023**, *7*, 511. [CrossRef]
14. Guo, X.; Diao, P.; Xu, D.; Huang, S.; Yang, Y.; Jin, T.; Wu, Q.; Xiang, M.; Zhang, M. CuO/Pd Composite Photocathodes for Photoelectrochemical Hydrogen Evolution Reaction. *Int. J. Hydrogen Energy* **2014**, *39*, 7686–7696. [CrossRef]
15. Oudah, M.H.; Hasan, M.H.; Abd, A.N. Synthesis of Copper Oxide Thin Films by Electrolysis Method Based on Porous Silicon for Solar Cell Applications. *IOP Conf. Ser. Mater. Sci. Eng.* **2020**, *757*, 012051–012058. [CrossRef]
16. Ashkarran, A.A.; Hamidinezhad, H.; Haddadi, H.; Mahmoudi, M. Double-Doped TiO_2 Nanoparticles as an Efficient Visible-Light-Active Photocatalyst and Antibacterial Agent under Solar Simulated Light. *Appl. Surf. Sci.* **2014**, *301*, 338–345. [CrossRef]
17. Raizada, P.; Sudhaik, A.; Patial, S.; Hasija, V.; Parwaz Khan, A.A.; Singh, P.; Gautam, S.; Kaur, M.; Nguyen, V.H. Engineering Nanostructures of CuO-Based Photocatalysts for Water Treatment: Current Progress and Future Challenges. *Arab. J. Chem.* **2020**, *13*, 8424–8457. [CrossRef]
18. Zindrou, A.; Belles, L.; Deligiannakis, Y. Cu-Based Materials as Photocatalysts for Solar Light Artificial Photosynthesis: Aspects of Engineering Performance, Stability, Selectivity. *Solar* **2023**, *3*, 87–112. [CrossRef]
19. Aguirre, M.E.; Zhou, R.; Eugene, A.J.; Guzman, M.I.; Grela, M.A. Cu_2O/TiO_2 Heterostructures for CO2 Reduction through a Direct Z-Scheme: Protecting Cu2O from Photocorrosion. *Appl. Catal. B Environ.* **2017**, *217*, 485–493. [CrossRef]
20. Toe, C.Y.; Scott, J.; Amal, R.; Ng, Y.H. Recent Advances in Suppressing the Photocorrosion of Cuprous Oxide for Photocatalytic and Photoelectrochemical Energy Conversion. *J. Photochem. Photobiol. C Photochem. Rev.* **2019**, *40*, 191–211. [CrossRef]
21. Feinberg, H.; Hanks, T.W. Polydopamine: A Bioinspired Adhesive and Surface Modification Platform. *Polym. Int.* **2022**, *71*, 578–582. [CrossRef]
22. Wang, H.; Jing, L.; Varamesh, A.; Yan, Y.; Zhang, H.; Gao, Q.; Hu, J. Application of Polydopamine-Based Photocatalysts in Energy and Environmental Systems. *Photocatal. Res. Potential* **2023**, *1*, 10007. [CrossRef]
23. Shi, J.L.; Lang, X. Assembling Polydopamine on TiO_2 for Visible Light Photocatalytic Selective Oxidation of Sulfides with Aerial O_2. *Chem. Eng. J.* **2020**, *392*, 123632–123645. [CrossRef]
24. Wang, T.; Xia, M.; Kong, X. The Pros and Cons of Polydopamine-Sensitized Titanium Oxide for the Photoreduction of CO_2. *Catalysts* **2018**, *8*, 215. [CrossRef]
25. Aguilar-Ferrer, D.; Szewczyk, J.; Coy, E. Recent Developments in Polydopamine-Based Photocatalytic Nanocomposites for Energy Production: Physico-Chemical Properties and Perspectives. *Catal. Today* **2022**, *397–399*, 316–349. [CrossRef]
26. Kim, D.; An, J.; Surendran, S.; Lim, J.; Jeong, H.Y.; Im, S.; Young Kim, J.; Nam, K.T.; Sim, U. Synergistic Effect of Polydopamine Incorporated Copper Electrocatalyst by Dopamine Oxidation for Efficient Hydrogen Production. *J. Colloid Interface Sci.* **2023**, *650*, 1406–1414. [CrossRef] [PubMed]
27. d'Alessandro, N.; Coccia, F.; Vitali, L.A.; Rastelli, G.; Cinosi, A.; Mascitti, A.; Tonucci, L. Cu-ZnO Embedded in a Polydopamine Shell for the Generation of Antibacterial Surgical Face Masks. *Molecules* **2024**, *29*, 4512. [CrossRef] [PubMed]
28. Du, J.; Cullen, J.J.; Buettner, G.R. Ascorbic Acid: Chemistry, Biology and the Treatment of Cancer. *Biochim. Biophys. Acta-Rev. Cancer* **2012**, *1826*, 443–457. [CrossRef]
29. Costantino, F.; Kamat, P.V. Do Sacrificial Donors Donate H_2 in Photocatalysis? *ACS Energy Lett.* **2022**, *7*, 242–246. [CrossRef]
30. Ikuta, N.; Takizawa, S.Y.; Murata, S. Photochemical Reduction of CO_2 with Ascorbate in Aqueous Solution Using Vesicles Acting as Photocatalysts. *Photochem. Photobiol. Sci.* **2014**, *13*, 691–702. [CrossRef]
31. Slamet; Nasution, H.W.; Purnama, E.; Kosela, S.; Gunlazuardi, J. Photocatalytic Reduction of CO_2 on Copper-Doped Titania Catalysts Prepared by Improved-Impregnation Method. *Catal. Commun.* **2005**, *6*, 313–319. [CrossRef]

32. Tonucci, L.; Mascitti, A.; Ferretti, A.M.; Coccia, F.; d'Alessandro, N. The Role of Nanoparticle Catalysis in the Nylon Production. *Catalysts* **2022**, *12*, 1206. [CrossRef]
33. Coccia, F.; Tonucci, L.; Del Boccio, P.; Caporali, S.; Hollmann, F.; D'Alessandro, N. Stereoselective Double Reduction of 3-Methyl-2-Cyclohexenone by Use of Palladium and Platinum Nanoparticles in Tandem with Alcohol Dehydrogenase. *Nanomaterials* **2018**, *8*, 853. [CrossRef] [PubMed]
34. Yendrapati Taraka, T.P.; Gautam, A.; Jain, S.L.; Bojja, S.; Pal, U. Controlled Addition of Cu/Zn in Hierarchical CuO/ZnO p-n Heterojunction Photocatalyst for High Photoreduction of CO_2 to MeOH. *J. CO2 Util.* **2019**, *31*, 207–214. [CrossRef]
35. Yeroslavsky, G.; Lavi, R.; Alishaev, A.; Rahimipour, S. Sonochemically-Produced Metal-Containing Polydopamine Nanoparticles and Their Antibacterial and Antibiofilm Activity. *Langmuir* **2016**, *32*, 5201–5212. [CrossRef] [PubMed]
36. A'srai, A.I.M.; Razali, M.H.; Amin, K.A.M.; Osman, U.M. CuO/TiO_2 Nanocomposite Photocatalyst for Efficient MO Degradation. *Dig. J. Nanomater. Biostructures* **2023**, *18*, 1005–1124. [CrossRef]
37. Hernández-Alonso, M.D.; Fresno, F.; Suárez, S.; Coronado, J.M. Development of Alternative Photocatalysts to TiO_2: Challenges and Opportunities. *Energy Environ. Sci.* **2009**, *2*, 1231–1257. [CrossRef]
38. Gleißner, R.; Chung, S.; Semione, G.D.L.; Jacobse, L.; Wagstaffe, M.; Tober, S.; Neumann, A.J.; Gizer, G.; Goodwin, C.M.; Soldemo, M.; et al. Role of Oxidation–Reduction Dynamics in the Application of Cu/ZnO-Based Catalysts. *ACS Appl. Nano Mater.* **2023**, *6*, 8004–8016. [CrossRef]
39. Yang, J.; Xu, H.; Zhang, L.; Zhong, Y.; Sui, X.; Mao, Z. Lasting Superhydrophobicity and Antibacterial Activity of Cu Nanoparticles Immobilized on the Surface of Dopamine Modified Cotton Fabrics. *Surf. Coat. Technol.* **2017**, *309*, 149–154. [CrossRef]
40. Si, Y.; Zhang, X.; Liang, T.; Xu, X.; Qiu, L.; Li, P.; Duo, S. Facile In-Situ Synthesis of 2D/3D g-C_3N_4/Cu_2O Heterojunction for High-Performance Photocatalytic Dye Degradation. *Mater. Res. Express* **2020**, *7*, 015524–015532. [CrossRef]
41. Fang, Q.; Zhang, J.; Bai, L.; Duan, J.; Xu, H.; Cham-Fai Leung, K.; Xuan, S. In Situ Redox-Oxidation Polymerization for Magnetic Core-Shell Nanostructure with Polydopamine-Encapsulated-Au Hybrid Shell. *J. Hazard. Mater.* **2019**, *367*, 15–25. [CrossRef] [PubMed]
42. Wang, T.; Zhang, Q.; Li, J.; Xu, G.; Guo, N.; Song, P.; Xia, L. Polydopamine-Assisted In Situ Growth of AgNPs on Face Masks for the Detection of Pesticide Based on Surface-Enhanced Raman Scattering Spectroscopy. *Plasmonics* **2022**, *17*, 1743–1750. [CrossRef]
43. Ding, Y.H.; Floren, M.; Tan, W. Mussel-Inspired Polydopamine for Bio-Surface Functionalization. *Biosurface Biotribology* **2016**, *2*, 121–136. [CrossRef] [PubMed]
44. Kiyani, H.; Bamdad, M. Sodium Ascorbate as an Expedient Catalyst for Green Synthesis of Polysubstituted 5-Aminopyrazole-4-Carbonitriles and 6-Amino-1,4-Dihydropyrano[2,3-c]Pyrazole-5-Carbonitriles. *Res. Chem. Intermed.* **2018**, *44*, 2761–2778. [CrossRef]
45. Basak, S.; Shaik, L.; Chakraborty, S. Effect of Ultraviolet and Pulsed Light Treatments on Ascorbic Acid Content in Fruit Juices-A Review of the Degradation Mechanism. *Food Chem. Adv.* **2023**, *2*, 100333–100346. [CrossRef]
46. Ahmad, I.; Shaikh, R.H.; Khurshid, A.; Khurshid, A.; Anwar, Z. Photolysis of ascorbic acid in aqueous solution: A kinetic study. *Baqai J. Health Sci.* **2019**, *22*, 84–95.
47. Orozco-Saumell, A.; Mariscal, R.; Iglesias, J.; Maireles-Torres, P.; López Granados, M. Aqueous Phase Hydrogenation of Maleic Acid to Succinic Acid Mediated by Formic Acid: The Robustness of the Pd/C Catalytic System. *Sustain. Energy Fuels* **2022**, *6*, 5160–5176. [CrossRef]